ISSN 0097-8078, Water Resources, 2018, Vol. 45, No. 4, pp. 565–577. © Pleiades Publishing, Ltd., 2018.

HYDROPHYSICAL PROCESSES

Experimental and Numerical Investigation of the Flow Hydraulic in Gradual Transition Open Channels[1]

Adel Asnaashari[a], Amir Ahmad Dehghani[b], Ali Akbar Akhtari[c, *], and Hossein Bonakdari[c]

[a]*Civil Engineering, Hydraulic Structures, Razi University, Kermanshah, Iran*

[b]*Department of Water Engineering, Gorgan University of Agricultural Sciences and Natural Resources, Gorgan, Iran*

[c]*Department of Civil Engineering, Razi University, Kermanshah, Iran*

**e-mail: akhtari@razi.ac.ir*

Received December 29, 2015

Abstract—Channel expansions are common in both natural and artificial open channels. With increasing cross-sectional dimensions in an expansion, the flow decelerates. Due to separation of flow and subsequent eddy formation, a significant head loss is occurred along the transition. This study presents the results of experimental investigations on subcritical flow along the expansive transition of rectangular to trapezoidal channels. Also, a numerical simulation was developed using the finite volume method with Reynolds Stress turbulent model. Water surface profiles and velocity distributions of flow through the transition were measured experimentally and compared with the numerical results. Also, hydraulic efficiency of the transition and coefficient of energy head loss were calculated. The results show that with increasing the upstream Froude number, hydraulic efficiency of the transition and coefficient of energy head loss are decreased and increased, respectively. The results also showed the ability of numerical simulation for simulating the flow separation zones and bed shear stress along the transition for different inlet discharges and inflow Froude numbers.

Keywords: experimental investigation, gradual transition, flow hydraulic, hydraulic efficiency, flow separation zones, bed shear stress

DOI: 10.1134/S0097807818040036

INTRODUCTION

A channel transition is defined as a change in the direction of channel, the slope of bed level or cross-sectional area [7]. A more complicated case is the combination of the above-mentioned geometric features. Channel expansions are commonly encountered in both natural open channels and constructed hydraulics facilities. Examples include flow through subdivided channels between bridge piers and water flowing out of culverts. Channel expansions are worth investigating because they disturb the approaching flow and more importantly because they can cause significant energy losses [10]. When passing through an expansion the flow decelerates with a rising water surface and a corresponding increase in pressure. This condition creates an adverse pressure gradient and causes the main flow to potentially separate from the sidewalls of the expansion [10]. Abbott and Kline [1] observed asymmetric flow patterns on an expansion transition in their experimental investigations. They also found that the Reynolds numbers and turbulence intensities have no effect on flow pattern. Ramamurthy and Basak [14] conducted an experimental study of flow separation in an expansion gradual transition and the suppression of flow separation by fitting a simple hump at the channel bottom. They showed that both the angle of divergence and the length of transition relative to the inlet dimension have effects on flow separation. Mehta [9] observed the behavior of the mean flow pattern and the turbulent characteristics for two-dimensional flow through large, sudden expansions. The flow patterns become more asymmetric and unsteady with increasing expansion ratios. Nashta and Garde [12] presented the results of analytical and experimental investigations in channels with a sudden expansion for subcritical flow. Swamee and Basak [15] discussed an analytical method for the design of expansions that connect a rectangular channel section with a trapezoidal channel section for subcritical flow. They suggested that flow separation in the expansion and the associated energy losses were considerably reduced. Escudier et al. [5] conducted an experimental study of turbulent flow in a sudden expansion. They reported that the flow downstream of the expansion is asymmetric. Manica and Bortoli [8] considered laminar flow with low Reynolds number in a symmetric sudden expansion, numerically. Their results show that below a certain critical Reynolds number

[1] The article is published in the original.

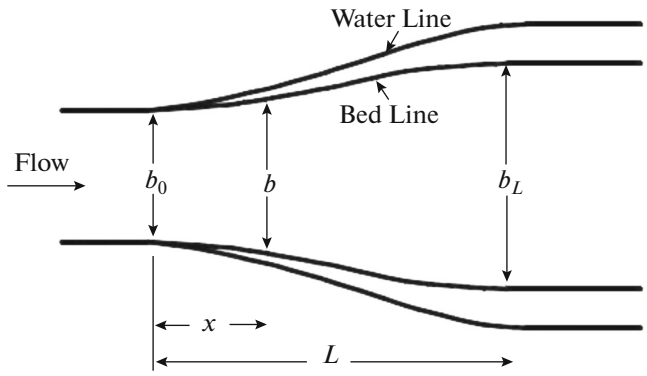

Fig. 1. Definition sketch: expansive transition of rectangular to trapezoidal.

(about 50); the flow pattern is symmetric around the channel central line. Alauddin and Basak [2] conducted the experimental approach to study flow separation in an abrupt expansion and further downstream. The purpose of their study was to design an expanding transition with minimum flow separation and hence small energy head losses. The velocity distributions of flow through the sudden as well as gradual expansion models were made, thus, a transition profile for expansion of flow with minimum separation evolved by streamlining the boundary shape of the transition. Najafi Nejad Nasser [10] observed coefficient of energy loss, water surface profiles and vertical distribution of water pressure in open channel expansions. Najmeddin [11] studied effects of different angles of divergence, crest height of the hump and the Froude number of subcritical flow on turbulent flow in open-channel expansions. Asnaashari et al. [3] investigated effect of inflow Froude number on flow pattern in channel expansive transitions, numerically. They show that with increasing the inflow Froude number, the strength of secondary current and turbulent kinetic energy along the transition are decreased and increased, respectively. In this study, an attempt is made to investigate the flow hydraulic in expansive transition of rectangular to trapezoidal open channel experimentally. Then, the effect of the different inflow Froude numbers on hydraulic efficiency of the transition and coefficient of energy head loss is considered along the channel expansion. Also, effect of inflow Froude numbers and inlet discharges on flow separation zones and bed shear stress at different cross sections is investigated. This study can be useful for practicing engineers to design transition more accurately.

DESIGN METHOD

Because of the importance of knowledge concerning expansions in rigid-bed channels, several investigators studied with different aspects of flow in expansion. In this study, for design of expansion transitions of rectangular to trapezoidal channels, method of Swamee and Basak [15] is used. A brief outline of this method is given as follows (Fig. 1).

The following equation is proposed for the bed-width profile.

$$b = \left[a\left(\frac{1-\xi}{\xi}\right)^{p} + 1 \right]^{-q}, \quad (1)$$

where a, p, and q are unknown positive numbers called transition parameters, L is transition length, x is distance from the transition inlet and $\zeta = x/L$. Eq. (1) satisfies the boundary conditions at the inlet and the outlet of the transition. The transition parameters were obtained by minimizing the function $E(a, p, q)$, given by [15]:

$$E(a,p,q) = \frac{100}{N}\sum_{j=1}^{N}\left|\left\{ b_i - \left[a\left(\frac{1-\xi_i}{\xi_i}\right)^{p} + 1 \right]^{-q} \right\}\right|, \quad (2)$$

where N is total number of bed-width profiles. The function $E(a, p, q)$ was minimized by grid-search algorithm. Such method yielded the following equation of the optimal bed-width profile [15]:

$$b = \left[2.52\left(\frac{1-\xi}{\xi}\right)^{1.35} + 1 \right]^{-0.775}. \quad (3)$$

Eq. (3) can be converted to the following dimensioned form [15]:

$$b = b_0 + (b_L - b_0)\left[2.52\left(\frac{L}{x} - 1\right)^{1.35} + 1 \right]^{-0.775}, \quad (4)$$

where b, b_0 and b_L are bed width of rectangular channel, bed width of transition and bed width of trapezoidal channel respectively. Analyzing a large number of optimal side-slope profiles, an equation for the design of rectangular to trapezoidal transitions was presented as [15]:

$$\frac{m}{m_L} = \xi^{1.23}, \quad (5)$$

where m and m_L are side slope of transition and side slope of trapezoidal channel respectively. Eq. (5) can be changed to the following directly usable form [15]:

$$m = m_L\left(\frac{x}{L}\right)^{1.23}. \quad (6)$$

EXPERIMENTAL SETUP

Experiments have been conducted in a re-circulating flume having a length of 11 m; width of 1 m and height of 0.8 m. The transition with a length of 1 m is connected to an upstream rectangular reach having length of 3 m and width of 0.25 m and a downstream trapezoidal reach having bed width of 0.4 m and the side slope of 1 : 1.

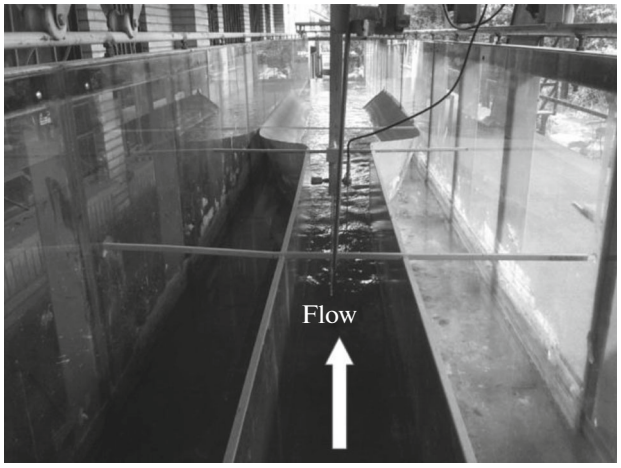

Fig. 2. Experimental setup for flow depth and velocity measurements.

The bed and sides of flume was made of glass supported by metal frame. Measurement of discharge was done using an ultrasonic flow meter located in supply pipe and checked with a sharp crested weir in downstream return channel. Water was supplied from a sump into the entrance tank. Water level in the flume was controlled by tail gate situated at the end of flume and measured with point gauge instrument with measurement accuracy of 0.01 mm. The channel was equipped with two rails on which an instrument carriage was mounted. The velocity is also measured with micro Moline instrument (Fig. 2).

To obtain the velocity distribution of flow through expansion and hence to evaluate the efficiency of transition, the (i) velocity at different points, and (ii) flow depth at different sections were to be measured. Velocities were measured at near surface, 0.20y, 0.40y, 0.60y, 0.80y and near bottom in the vertical. These measurements were made at a number of sections across the transition reach at 1/8, 3/8, 1/2, 5/8 and 7/8 times the width, (Fig. 3) and along the length of transition at inlet, mid-length, and outlet sections. The experiments were conducted with five different discharges, i.e. 10, 15, 20, 25 and 30 L/s. Table 1 shows range of flow hydraulic characteristics.

HYDRAULIC EFFICIENCY AND COEFFICIENT OF ENERGY HEAD LOSS

For finding the hydraulic efficiency, it is necessary to consider the velocity variation across the channel. Assuming that the flow is essentially in the direction of

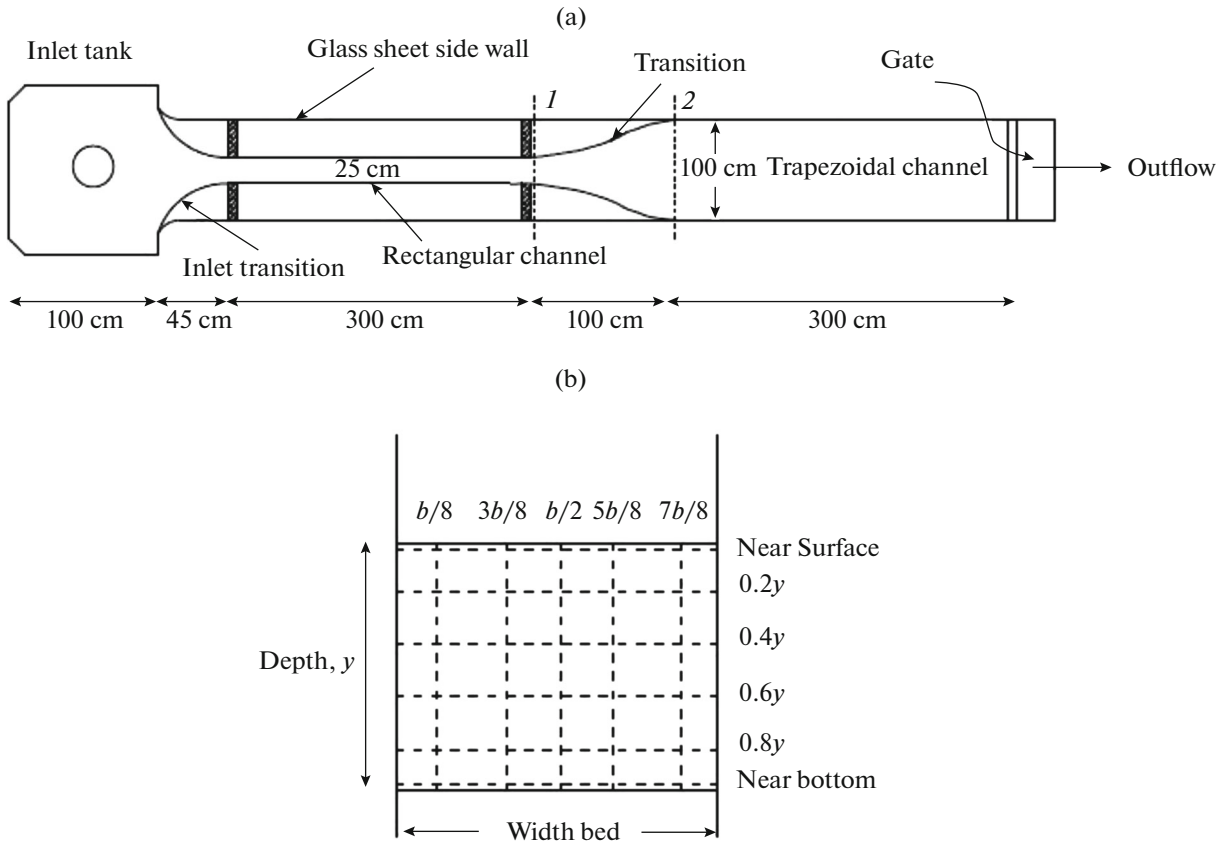

Fig. 3. Top view of flume (a) with the section showing the various points of velocity measurements (b).

Table 1. Range of flow hydraulic characteristics

Discharge (Q)	Upstream depth (y_0)	Inlet velocity (u_0)	Inlet Froude number (Fr_1)
10–30 L/s	69–243 mm	0.345–0.833 m/s	0.32–0.70

the axis of the transition, the hydraulic efficiency of the transition is defined by [4]:

$$\varepsilon = \frac{Q\rho g(y_2 - y_1)}{\left(\frac{1}{2}\rho Q V_1^2\right)\alpha_1 - \left(\frac{1}{2}\rho Q V_2^2\right)\alpha_2} = \frac{(y_2 - y_1)}{\left(\alpha_1 \frac{V_1^2}{2g} - \alpha_2 \frac{V_2^2}{2g}\right)}, \quad (7)$$

where, Q is inlet discharge, g is gravity acceleration, ρ is fluid density, y_1 and y_2 are depths of flow at sections 1 and 2, respectively, α_1 and α_2 are energy correction factors at inlet and outlet sections of the transition, respectively and V_1 and V_2 are average velocities at section 1 and 2, respectively.

Using the data for flow depth and local velocity, the flow area and average velocity at the sections were known, and thus energy correction factors were calculated. After then these data were used to evaluate the efficiency of transition. Energy loss coefficient is defined also as [10],

$$k_e = \frac{H_1 - H_2}{\frac{V_1^2}{2g}}. \quad (8)$$

In a horizontal channel, Eq. (8) becomes

$$k_e = \frac{E_1 - E_2}{\frac{V_1^2}{2g}} = \frac{\left(y_1 + \frac{V_1^2}{2g}\right) - \left(y_2 + \frac{V_2^2}{2g}\right)}{\frac{V_1^2}{2g}}, \quad (9)$$

where k_e is energy loss coefficient, g is gravity acceleration, y_1 and y_2 are depths of flow at sections 1 and 2, respectively and H_i is the total energy head equal to the sum of velocity head, elevation head and pressure head.

DESCRIPTION OF THE MODEL AND BOUNDARY CONDITIONS

For numerical simulation of the turbulent flow field, Fluent software with RSM turbulent model was used. Reynolds-averaged Navier–Stokes (RANS) equations are solved in addition of continuity equation. Quick and second Order Upwind schemes were used for solving momentums and turbulence equations, respectively Also, standard method was used for discritization of pressure equation. In the present study, Reynolds Stress Model with standard wall function was selected for numerical simulations of the turbulent flow. The volume of fluid (VOF) scheme is used for simulating free surface [16]. In the present study, the boundaries of the numerical model based on the nature of the experimental model were solid walls, inlet, outlet and free-surface. For air surface modeling, the pressure inlet boundary condition was used. To estimate the wall effects on the flow, empirical wall functions known as standard wall functions were used. Appropriate meshing of the computational domain is one of the important parameters in the model run time. The grid structure must be fine enough, especially near the wall boundaries and the expansion, which is the region of rapid variation. The generated mesh is non-uniform. The cells numbers in the x, y and z directions in upstream channel are 60 × 15 × 21, in expansion transition are 30 × 15 × 21 and in downstream channel are 50 × 15 × 21.

EXPERIMENTAL OBSERVATIONS AND RESULTS

As mentioned, for finding the efficiency, it is necessary to consider the velocity values and water level along the channels. Tables 2 and 3 show measured water level along the centre line of the channels for different Froude numbers and Measured velocities at different depths, respectively. Also, measured velocities at near water surface for $Fr_1 = 0.47$ are presented in Fig. 4.

As seen in Table 2, the flow depth increases along the expansive transition. $Fr_1 = 0.70$ has the maximum water surface slope and $Fr_1 = 0.32$ has the minimum slope. It is possible that the increase in the water surface slope is related to the increasing value for the Froude number and with increasing the inlet Froude number, water surface slope is increased. According to Fig. 4, excepting $Q = 10$ L/s flow was never symmetrical with respect to the centre line of the channel. The maximum velocity line coincided with the centre line of the channel, for a short length after entry. Thereafter, it shifted to the side to which the main flow attached.

For discharges above 10 L/s, velocities at transition corners are negative and close to zero that indicate flow separation zones are formed there. Also, along the transition with approaching to the transition outlet, velocities values are decreased. The hydraulic efficiency of the transition and energy loss coefficient along the transition has been shown in Figs. 5 and 6, respectively.

As shown in Fig. 5, the overall hydraulic efficiency of the transition increases from $Q = 30$ L/s to $Q = 10$ L/s, and these are 30.36, 35.45, 39.98, 48.32 and 60.83%, respectively. Efficiency of the $Q = 10$ L/s is the highest among the models, and it is 60.83%. With

Table 2. Measured water level along the centre line of the channels

Q, L/s	Fr_1	y at inlet, mm	y at $L/6$, mm	y at $L/3$, mm	y at $L/2$, mm	y at $4L/6$, mm	y at $5L/6$, mm	y at outlet, mm
10	0.32	113.49	114.79	115.69	115.98	116.15	116.58	116.99
	0.40	97.06	97.82	98.75	99.39	99.64	100.45	101.10
	0.47	84.64	86.20	87.15	87.35	87.58	88.33	89.04
	0.55	76.20	78.81	79.95	80.91	81.06	81.32	81.80
	0.63	68.02	69.64	71.83	72.64	73.76	74.05	74.82
	0.70	63.01	65.66	67.85	68.66	69.28	69.87	70.71
20	0.32	183.18	183.46	185.11	185.73	186.18	186.90	187.22
	0.40	156.61	157.89	159.13	159.82	159.63	160.51	160.79
	0.47	138.88	140.18	141.45	141.98	142.61	143.22	143.84
	0.55	123.75	125.04	126.88	127.83	128.45	129.01	129.38
	0.63	111.32	113.21	114.98	115.82	116.44	117.39	118.09
	0.70	103.04	104.26	106.33	108.69	109.30	110.27	110.92

Table 3. Measured velocities at different depths for $Fr_1 = 0.47$

Q, L/s	Fr_1	Section	At depth	Velocity (u_x) in m/s				
				At $b/8$	At $3b/8$	At b/2	At $5b/8$	At $7b/8$
20	0.47	Inlet	$0.1y$	0.575	0.654	0.686	0.665	0.581
			$0.2y$	0.580	0.665	0.702	0.679	0.588
			$0.4y$	0.568	0.648	0.683	0.660	0.576
			$0.6y$	0.538	0.620	0.653	0.628	0.549
			$0.8y$	0.511	0.589	0.621	0.598	0.522
			$0.9y$	0.477	0.557	0.586	0.572	0.488
20	0.47	Mid-length	$0.1y$	0.325	0.508	0.535	0.557	0.349
			$0.2y$	0.343	0.516	0.548	0.565	0.369
			$0.4y$	0.320	0.479	0.484	0.532	0.354
			$0.6y$	0.286	0.432	0.441	0.482	0.328
			$0.8y$	0.183	0.397	0.405	0.438	0.301
			$0.9y$	0.095	0.328	0.344	0.377	0.269
20	0.47	Outlet	$0.1y$	0.235	0.379	0.442	0.461	0.252
			$0.2y$	0.248	0.388	0.458	0.469	0.267
			$0.4y$	0.231	0.361	0.439	0.448	0.256
			$0.6y$	0.207	0.323	0.391	0.419	0.237
			$0.8y$	0.133	0.284	0.344	0.381	0.218
			$0.9y$	0.069	0.211	0.317	0.339	0.195

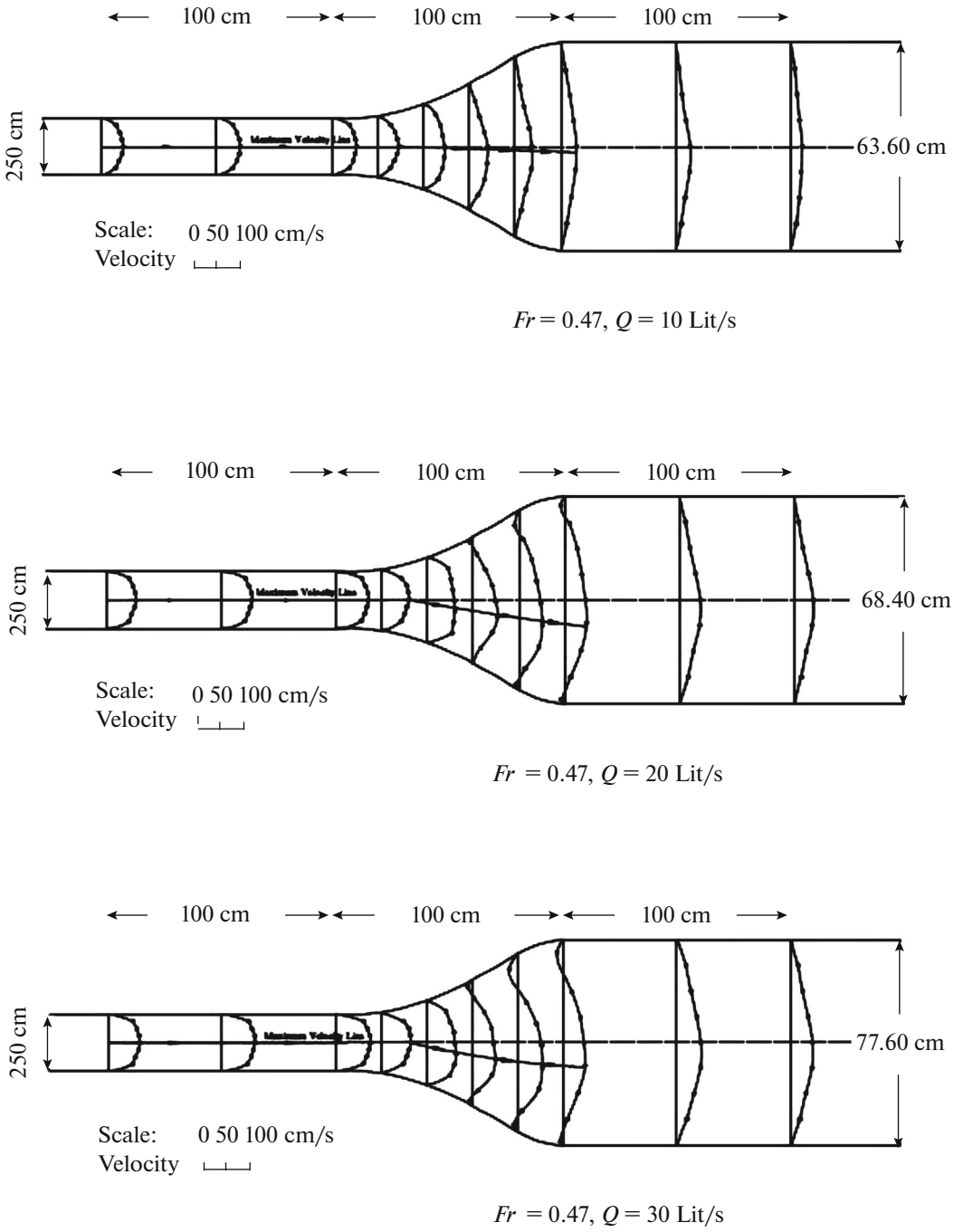

Fig. 4. Velocity distributions across the width and along the length of transition at near the water surface.

increasing the inlet Froude number, efficiency of the transition is decreased as from $Fr_1 = 0.47$ to $Fr_1 = 0.70$, due to increasing the water surface slope, decreasing process of efficiency decreases. Also, from $Fr_1 = 0.32$ to $Fr_1 = 0.47$ by increasing the inlet discharge, slope down efficiency is decreased. As shown in Fig. 6, with increasing the inlet Froude number, energy loss coefficient is increased. Maximum value of energy loss coefficient is equal to 0.609 and occurs at $Fr_1 = 0.70$. Also, with increasing the inlet discharge, energy loss coefficient is increased. Figure 7 compares simulated water surface profiles with the experimental data along the transition for inlet Froude numbers and Q = 20 L/s.

As seen Fig. 7, a good agreement is found between numerical simulation of the water surface profile and

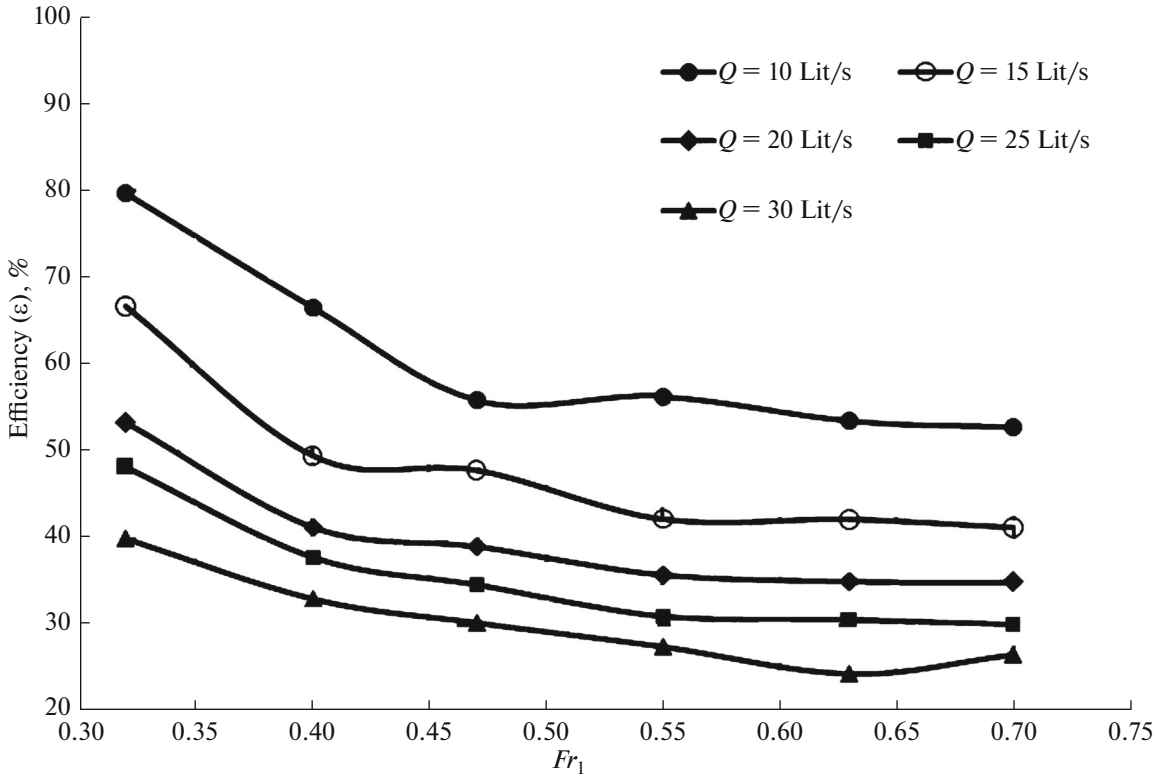

Fig. 5. Hydraulic efficiency of the transition for different inlet discharges.

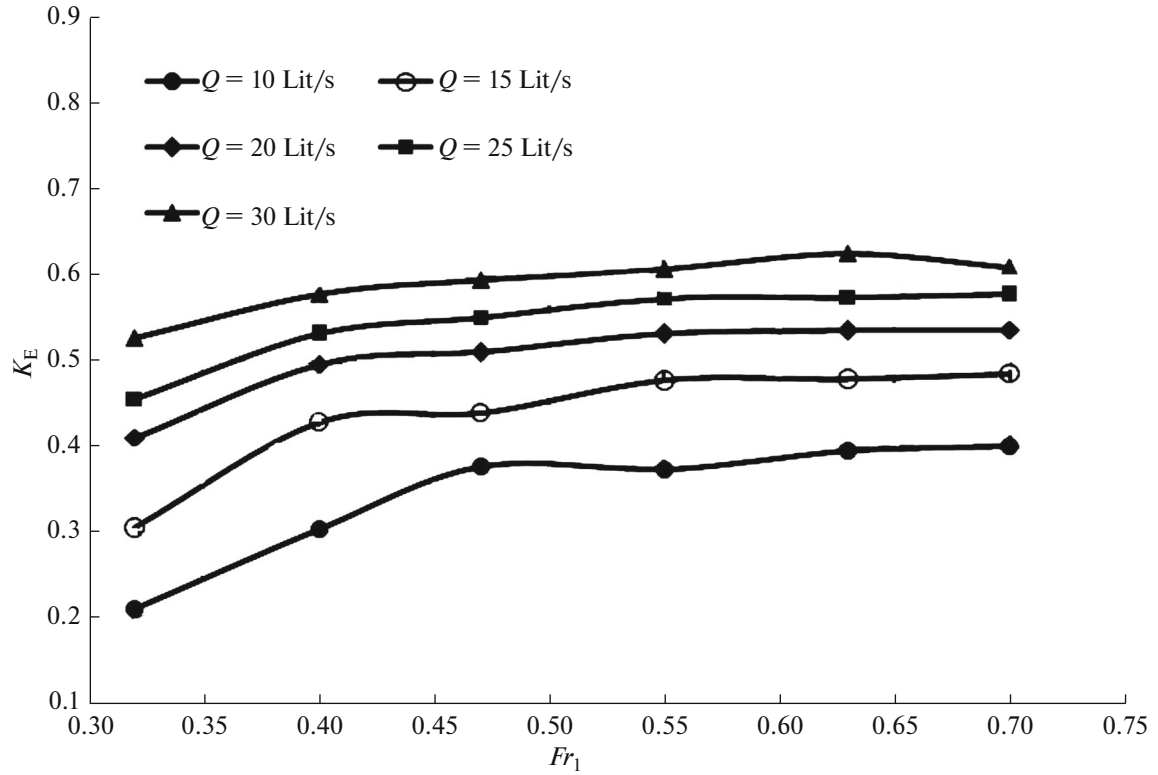

Fig. 6. Energy loss coefficient along the transition for different Froude numbers.

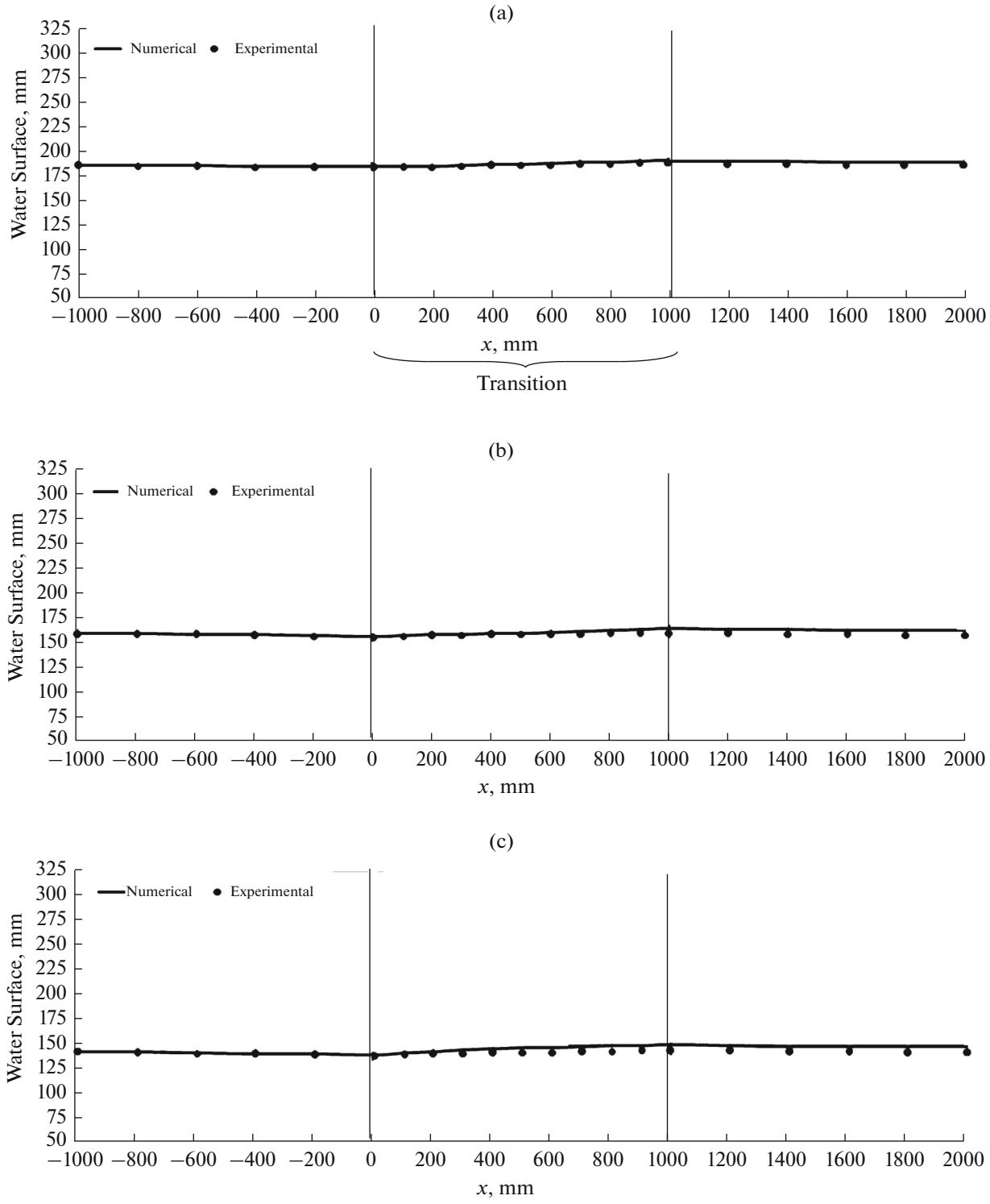

Fig. 7. Comparison of simulated water surface with experimental results for (a) $Fr_1 = 0.32$, (b) $Fr_1 = 0.40$, (c) $Fr_1 = 0.47$, (d) $Fr_1 = 0.55$ and (e) $Fr_1 = 0.63$.

experimental results. For error percentage calculation obtained from the comparison of the measured and calculated values, Root Mean Square Error method (RMSE) is used. The mean error percentage obtained from the comparison of the numerical results with the experimental results for $Fr_1 = 0.32$ to $Fr_1 = 0.70$ are 0.458, 0.676, 0.895, 1.795, 1.310 and 0.866%, respectively. Figure 8 shows the simulated and measured lon-

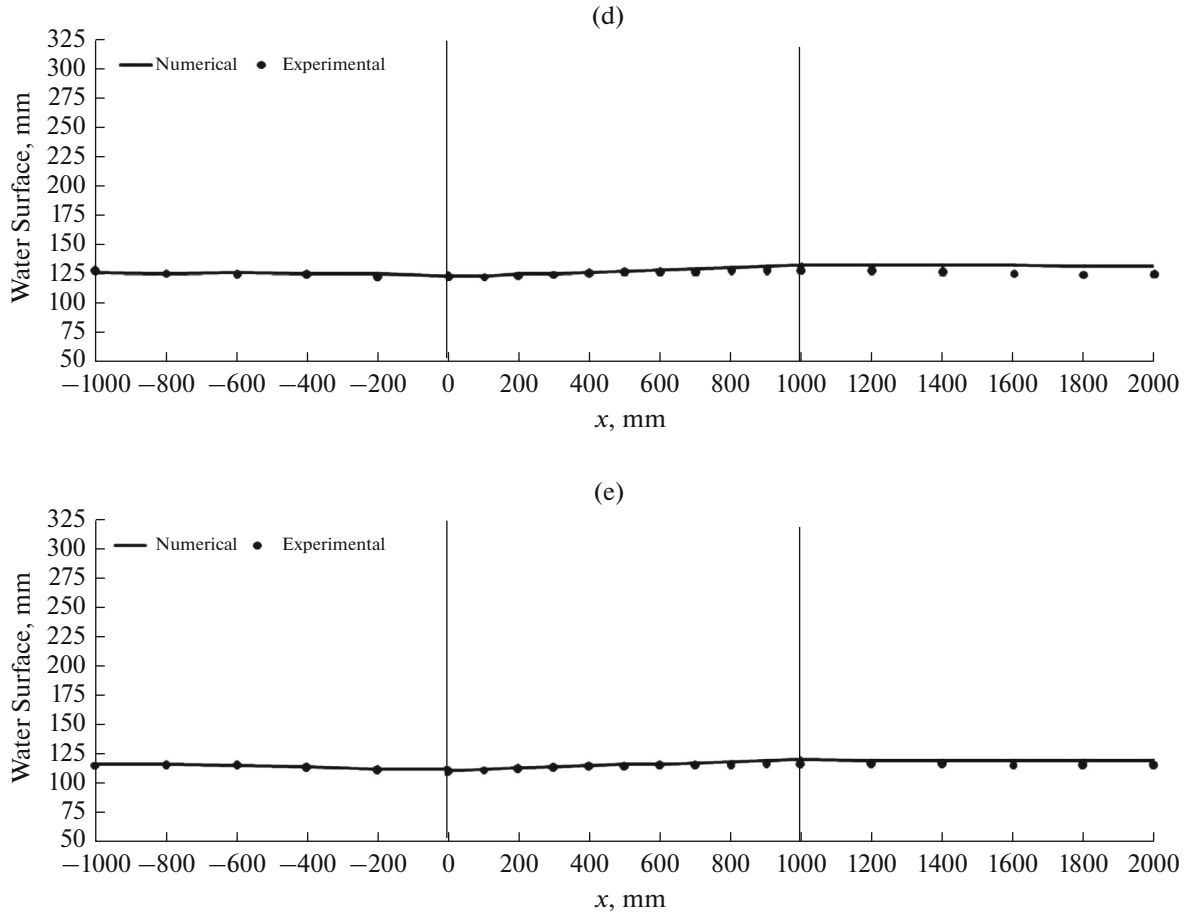

Fig. 7. (Cont.).

gitudinal velocity profiles (u_x) in different cross sections of the transition for Q = 10 L/s and Fr_1 = 0.47. Velocities values are dimensionless by inlet flow velocity (u_0).

As seen Fig. 8, similar to measured results, with approaching to the transition outlet, longitudinal velocity decreases. Also, a good agreement is found between numerical simulation of the velocity profiles and experimental results. The mean error percentage obtained from the comparison of the numerical results with the experimental results at transition inlet, transition middle and transition outlet are 4.962, 6.234 and 4.575%, respectively. Consequently, for evaluation of the flow separation zone in transition, Fig. 9 shows streamline at near the water surface for Fr_1 = 0.47 and different discharges 10, 15, 20 and 25 L/s.

As seen in Fig. 9, inlet discharge of expansion has an effect on flow pattern in expansion. As shown in Fig. 9, by increasing the inlet discharge of expansion, the length and width of the flow separation zone are increased. In Q = 10 L/s to Q = 25 L/s, the lengths of separation zone are obtained as 0.16, 0.62, 0.67 and 0.98 m, respectively. Also, from Q = 10 L/s to Q = 25 L/s, width of separation zone is increased from 0.039 to 0.25 m. Figure 10 shows contours of the bed shear stress at various cross sections along the transition for inflow Froude numbers and inlet discharge of 20 L/s.

As seen in Fig. 10, bed shear stress decreases from transition inlet toward middle and increases at end of the transition. Maximum of the bed shear stress is occurred at transition inlet and middle and for Fr_1 = 0.32, Fr_1 = 0.47, Fr_1 = 0.55 and Fr_1 = 0.63 are obtained 0.388, 0.422, 0.715 and 1.072 N/m^2, respectively. Also, with increasing the inflow Froude number, bed shear stress is increased as from Fr_1 = 0.32 to Fr_1 = 0.63, the average bed shear stress is increased about 2.67 times.

CONCLUSIONS

This study presents the results of experimental investigations on subcritical flow through transition in rectangular to trapezoidal channel. Then, flow numerical simulation was performed in transition and RANS equations were solved by Finite-Volume Method. The flow calculations were performed in the

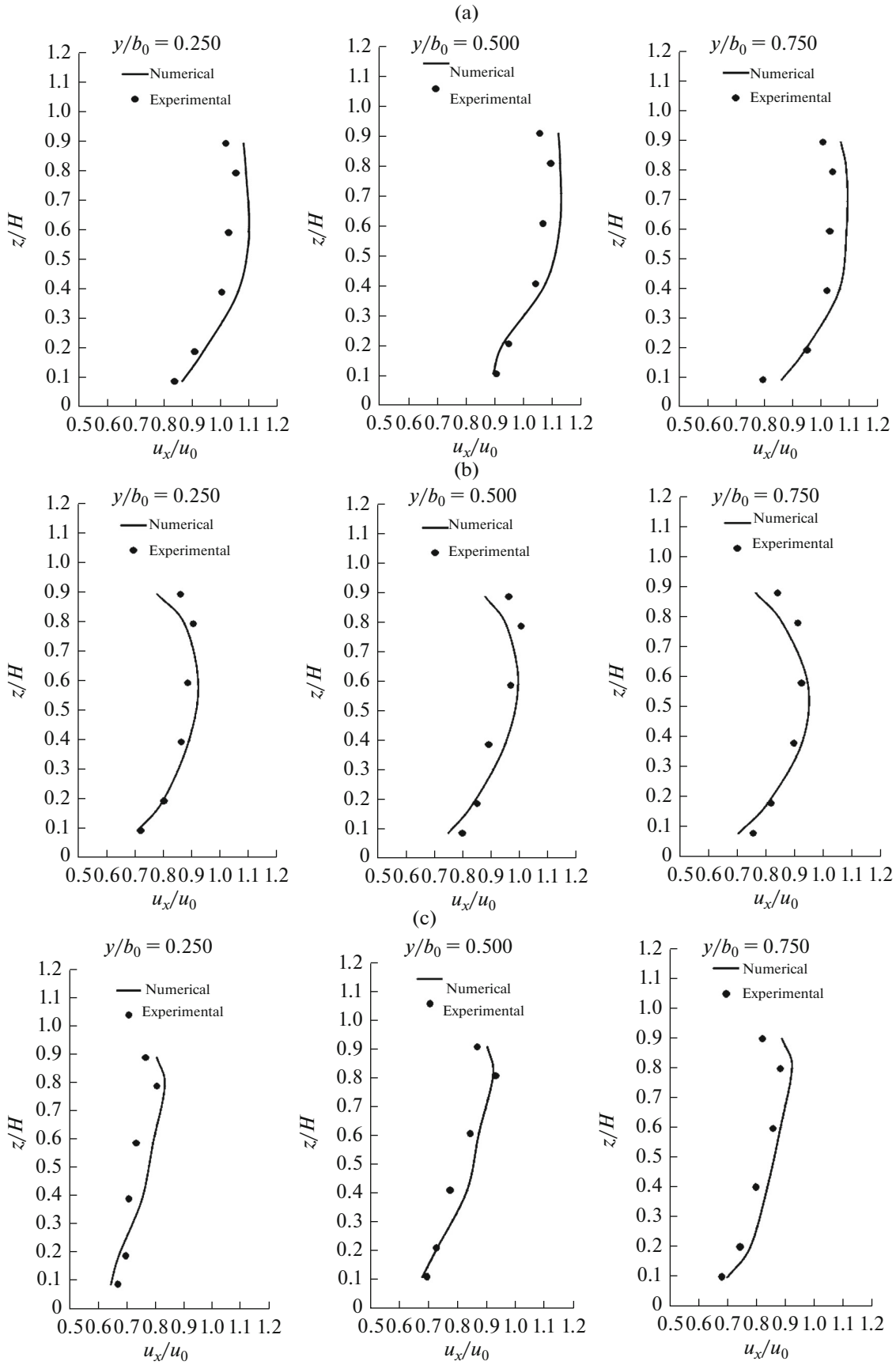

Fig. 8. Simulated longitudinal velocity profiles at transition inlet (a), transition middle (b) and transition outlet (c).

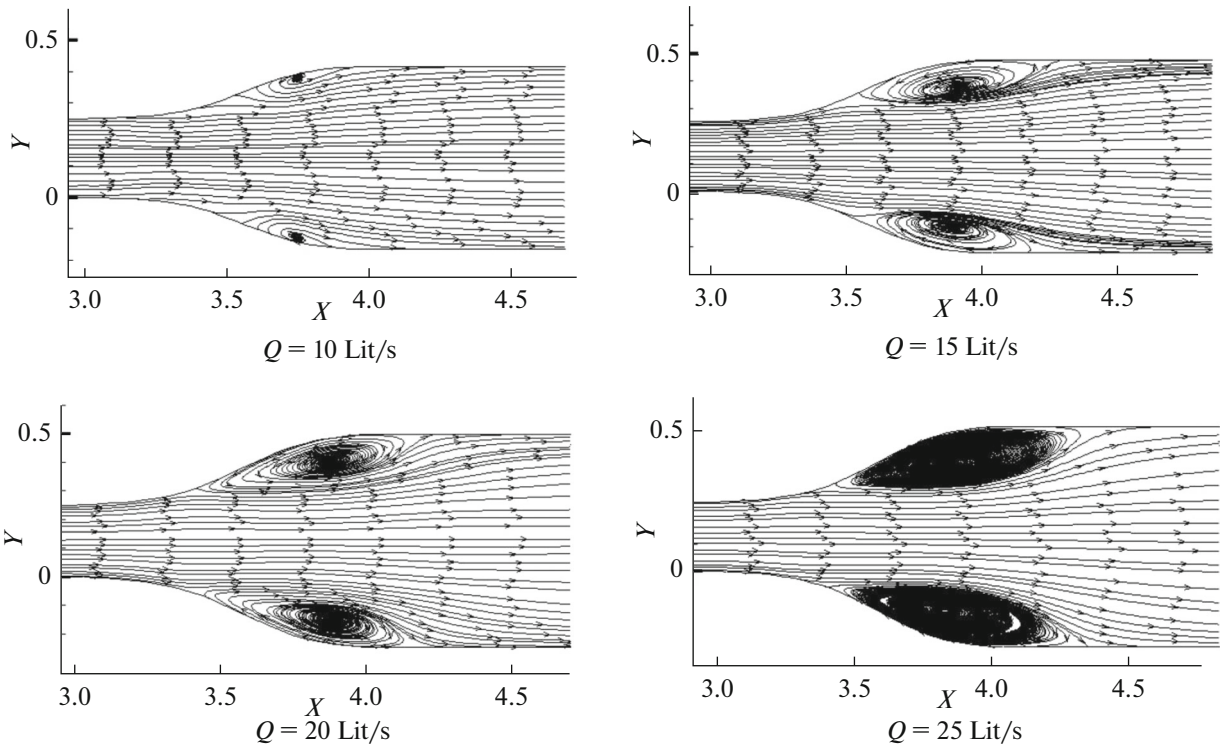

Fig. 9. Streamlines at near the water surface for different discharges.

three dimensional model using RSM turbulence model. The results showed a good agreement between numerical and experimental results. The results of this study are as follows:

The measured flow depth increases along the expansive transition. It is possible that the increase in the water surface slope is related to the increasing value for the Froude number. Water surface profiles in the expansion were compared with experimental results and good agreement was found between them.

With increasing the inlet Froude number, hydraulic efficiency of the transition was decreased. Due to increasing the water surface slope, decreasing process of efficiency was decreased. Also, by increasing the inlet discharge and Froude number, energy loss coefficient was increased.

The flow pattern along the expansion was asymmetric (except Q = 10 L/s). The maximum velocity line coincided with the centre line of the channel, for a short length after entry. Thereafter, it shifted to the side to which the main flow attached.

For discharges above 10 L/s, velocities at transition corners were negative and close to zero that indicate flow separation zones are formed there. Also, a good agreement was found between numerical simulation of the velocity profiles and experimental results.

Inlet discharge of expansion has an effect on flow pattern in expansion. As by increasing the inlet discharge of expansion, the length and width of the flow separation zone are increased.

Bed shear stress decreases from transition inlet toward middle and increases at end of the transition. Maximum of the bed shear stress was occurred at transition inlet and middle. Also, with increasing the inflow Froude number, bed shear stress was increased.

NOTATION

The following symbols are used in this paper:

u_0	average inlet velocity
L	transition length
b_0	bed width of rectangular channel
b	bed width of transition
b_L	bed width of trapezoidal channel
m	side slope of transition
m_L	side slope of trapezoidal channel
V_1	average velocity at section 1
V_2	average velocity at section 2
y_1	depth of flow at section 1
y_2	depth of flow at section 2
α_1	energy correction factor at transition inlet
α_2	energy correction factor at transition outlet
z	measured point height
ε	efficiency

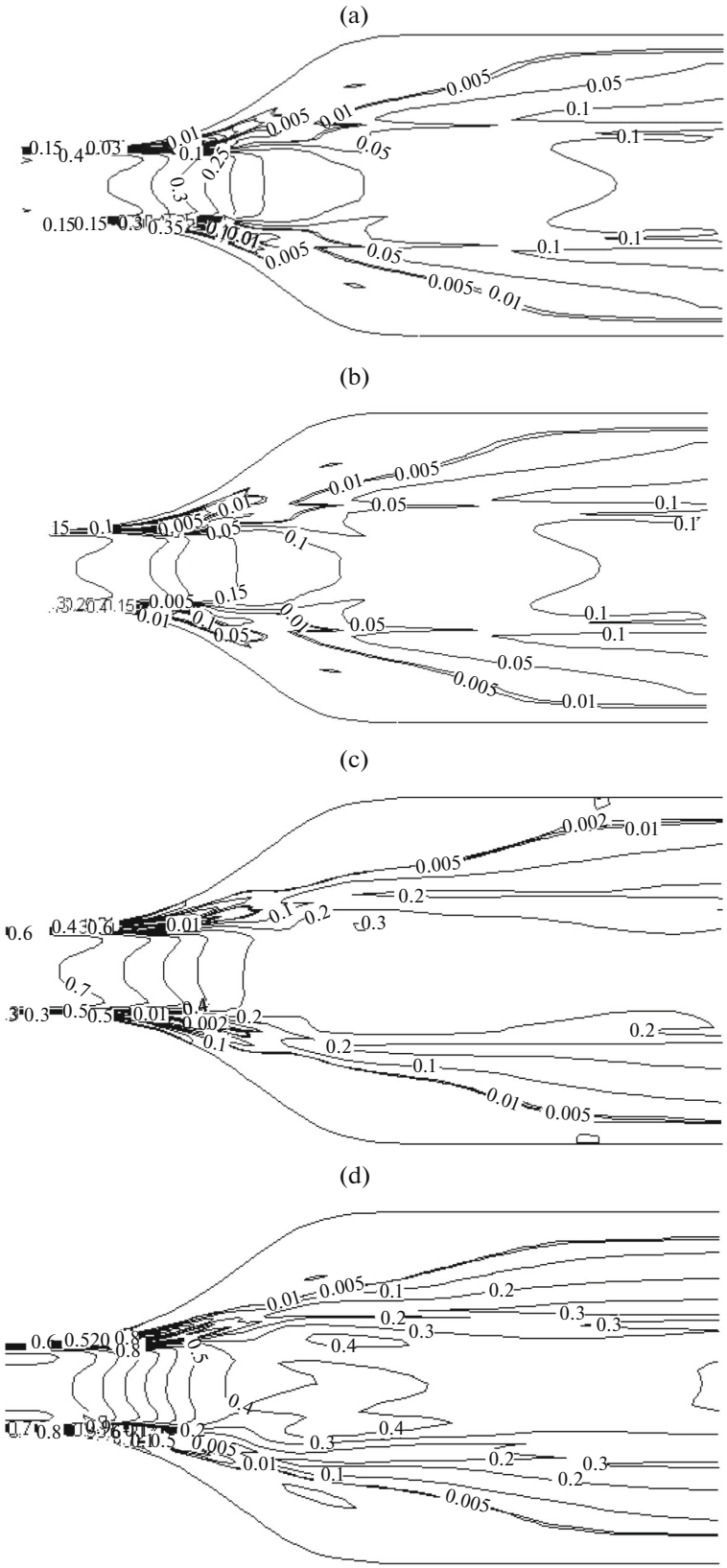

Fig. 10. Contours of simulated bed shear stress for (a) $Fr_1 = 0.32$, (b) $Fr_1 = 0.47$, (c) $Fr_1 = 0.55$ and (d) $Fr_1 = 0.63$.

k_e energy loss coefficient

H_i total energy head

Fr_1 inflow Froude number

Q inlet discharge

REFERENCES

1. Abbott, D.E. and Kline, S.J., Experimental investigation of subsonic turbulent flow over single and double backward facing steps, *J. Basic Eng.*, 1962, vol. 84, no. 3, pp. 317–325.
2. Alauddin, M. and Basak, B.C., Development of an expansion transition in open channel sub-critical flow, *J. Civil Engin.*, 2006, vol. 34, no. 2, pp. 91–101.
3. Asnaashari, A., Akhtari, A., Dehghani, A., and Bonakdari, H., Effect of inflow Froude number on flow pattern in channel-expansive transitions, *J. Irrig. Drain. Div., Am. Soc. Civ. Eng.*, 2015, ISSN: 0733-9437.
4. Basak, B.C. and Alauddin, M., Efficiency of an expansive transition in an open channel subcritical flow, *DUET J., Dhaka Univ. Engin. & Technol.*, 2010, vol. 1, no. 1, pp. 27–32.
5. Escudier, M.P., Oliveira, P.J., and Poole, R.J., Turbulent flow through a plane sudden expansion of modest aspect ratio, *J. Phys. Fluids–AIP*, 2002, vol. 14, no. 10, pp. 3641– 3654.
6. Haque, A., Some characteristics of open channel transition flow, *MSc Thesis*, Civil Engineering, Concordia University, 2008.
7. Henderson, F.M., *Open channel flow*, Prentice-Hall, Inc., Upper Saddle River, Macmillan, University of Michigan, 1966.
8. Manica, R. and Bortoli, A.L., Simulation of incompressible non-Newtonian flows through channels with sudden expansion using the power-law model, *Tema Tend. Math. Apl. Comput.*, 2003, vol. 4, no. 3, pp. 333–340.
9. Mehta, P.R., Separated flow through large sudden expansions, *J. Irrig. Drain. Div., Am. Soc. Civ. Eng.*, 1981, vol. 107, no. 4, pp. 451–460.
10. Najafi Nejad Nasser, A., An experimental investigation of flow energy losses in open-channel expansions, *MSc Thesis*, Civil Engineering, Concordia Univ., 2011.
11. Najmeddin, S., CFD modeling of turbulent flow in open-channel expansions, *MSc Thesis*, Civil Engineering, Concordia Univ., 2012.
12. Nashta, C.F. and Grade, R.J., Subcritical flow in rigid-bed open channel expansions, *J. Hydraulic Res.*, 1988, vol. 26, no. 1, pp. 49–65.
13. Olsen, N.R.B., *Numerical Modelling and Hydraulics*, Department of hydraulic and environmental engineering, Norwegian University of Science and Technology, 2008, ISBN: 82-7598-074-7, pp. 1–157.
14. Ramamurthy, A.S., Basak, S., and Rao, P.R., Open channel expansions fitted with local hump, *J. Hydraul. Div., Am. Soc. Civ. Eng.*, 1970, vol. 96, no. 5, pp. 1105–1113.
15. Swamee, P.K. and Basak, B.C., Design of trapezoidal expansive transitions, *J. Irrig. Drain. Div., Am. Soc. Civ. Eng.*, 1992, vol. 118, no. 1, pp. 61–73.
16. User Manual, Fluent Inc., 2006.